J Solid State Electrochem (2008) 12:57–62
DOI 10.1007/s10008-007-0337-x

ORIGINAL PAPER

Battery performance of nanostructured lithium manganese oxide synthesized by ultrasonic spray pyrolysis at elevated temperature

Zhumabay Bakenov · Masataka Wakihara · Izumi Taniguchi

Received: 6 March 2007 / Revised: 23 March 2007 / Accepted: 13 April 2007 / Published online: 4 May 2007

Abstract Nanostructured lithium manganese oxide with spherical particles was synthesized via ultrasonic spray pyrolysis technique. The material shows a pronounced stability upon prolonged cycling at room temperature at high charge–discharge rates up to 10C. The electrochemical performance of the cell at elevated temperature was remarkably improved by addition of $AlPO_4$ to the electrolyte. The AC impedance spectroscopy study showed the interface stabilization by the $AlPO_4$ additives and the suppression of the interface impedance development upon prolonged cycling.

Keywords Lithium battery · Nanostructured lithium manganese oxide · Ultrasonic spray pyrolysis · Elevated temperature performance

Introduction

Lithium-ion batteries (LIBs) are one of the great successes of modern materials electrochemistry [1]. Rechargeable LIBs have become the key components for wide range of portable electronic and most promising energy supplier for electricity-powered transport. Secondary lithium-ion batteries have been shown to be preferable for implantable systems due to their high energy density, long cycle life, and relatively small change in temperature during cycling [2]. These batteries pack three times more energy into a given volume than a conventional alkaline battery and can be recharged an almost unlimited number of times [3].

The major factors limiting wider application of lithium-ion batteries remain to be cost, which is due to the use of expensive electrode materials and lithium salts, environmental issues coming mainly from application of high-toxic electrode materials, and safety arising from application of flammable organic solutions in the structure of electrolytes. New developments are taking place to address these limitations [4, 5] in all aspects of batteries, including materials for anodes, cathodes, electrolytes, and design.

The cathode is a key component in the lithium-ion batteries, and the $LiCoO_2$ and $LiNiO_2$ are currently used as the main cathode materials. The use of these high-cost, toxic and unsafe cathode materials restricts the development of zero-emission types of cars based on these batteries. Therefore, lithium manganese oxide $LiMn_2O_4$ with spinel structure is one of the most promising candidates for cathode materials from the economical, safety and environmental points of view, and it has been under intensive investigation by many researchers [6–12]. However, $LiMn_2O_4$ suffers from drastic capacity fading upon prolonged cycling [4, 6], especially at elevated temperatures, which restricts its commercialization. Several possible factors have been ascribed to be the sources of capacity loss such as the Jahn–Teller distortion and the coexistence of unstable phases [13, 14]. Another important factor of capacity loss is the manganese dissolution during the battery operation [15, 16].

Z. Bakenov · M. Wakihara (✉)
Department of Applied Chemistry,
Tokyo Institute of Technology,
2-12-1 Ookayama, Meguro-ku,
Tokyo 152-8552, Japan
e-mail: mwakihar@o.cc.titech.ac.jp

I. Taniguchi
Department of Chemical Engineering,
Tokyo Institute of Technology,
2-12-1 Ookayma, Meguro-ku,
Tokyo 152-8552, Japan

Surface modification via coating the $LiMn_2O_4$ surface by oxides [17–26] has been considered as a promising technique to overcome the lithium manganese oxide electrode drawbacks. Gnanaraj et al. [25] have reported the surface modification of $LiMn_2O_4$ with Al_2O_3 by a melting impregnation method. The nano-Al_2O_3 particle coating improved the capacity retention of the spinel material. In [27, 28], the researchers have reported the preparation of the $AlPO_4$-coated $LiCoO_2$ cathode materials that exhibited superior electrochemical performance and thermal stability compared with bare material and Al_2O_3-coated cathodes. However, there were no studies on the electrochemical performance of the surface modification of nanostructured spherical particle $LiMn_2O_4$ by $AlPO_4$.

The improvement of charge–discharge performance of the pristine $LiMn_2O_4$ by adopting the simplest synthesis route is crucial. Among the other synthesis methods, the ultrasonic spray pyrolysis technique is considered as a single-step method to prepare nanostructured spherical oxide powders with narrow particle size distribution and homogeneous composition [29–31]. We have previously reported [29, 30] that the partially substituted nanostructured lithium manganese oxides with spherical particles have exhibited the electrochemical performance superior to the materials prepared by soft chemistry methods. Later, Park et al. [32] reported the preparation of nanostructured lithium manganese oxide via ultrasonic spray pyrolysis technique. It was shown [32] that due its nanostructured features, the synthesized material exhibits superior room temperature performance to the conventional microstructured one in 3-V range; however, in 4-V region, the nanostructured material has lower capacity than the microstructured counterpart.

In this study, we report the electrochemical performance of the parent nanostructured $LiMn_2O_4$ electrode with spherical particles synthesized via ultrasonic spray pyrolysis technique and its further improvement at elevated temperature via the electrode/electrolyte interface modification by the addition of aluminum phosphate to electrolyte.

Experimental

Lithium manganese oxide $LiMn_2O_4$ was prepared by ultrasonic spray pyrolysis technique. Schematic diagrams of the experimental apparatus and powder preparation procedure have been described elsewhere [29–31].

Precursor solution was prepared by dissolving stoichiometric amounts of $LiNO_3$ (98% purity) and $Mn(NO_3)_2{\cdot}6H_2O$ (98% purity) in distilled water. For all experiments, the total cation concentration was 0.90 mol/dm^3. All chemicals were purchased from Wako Pure Chemical Industries, Tokyo, Japan.

The precursor solution was atomized at a frequency of 1.7 MHz by the ultrasonic nebulizer (1.7 MHz, Omron, Model NE-U12). The sprayed droplets were carried to the laminar flow aerosol reactor (a high-quality quartz tube of 90 mm inner diameter and 1.86 m length), heated in air by an electric furnace at 800 °C, and converted into solid oxide particles through the process of evaporation of a solvent, precipitation of solute, drying, pyrolysis, and sintering within the laminar flow aerosol reactor. The resulting particles were collected at the reactor end by the electrostatic precipitator at 150 °C.

The crystalline phases of samples were determined by X-ray diffraction (XRD; Phillips, PW1700) with a scan speed of 2.4°/min for crystal analysis ranging from 4° to 70° and 0.6°/min for the lattice parameter measurements ranging from 40° to 90°, respectively. The crystallite size was estimated using Scherrer's formula from a (400) plane peak of the samples. The particle morphology was examined by field emission–scanning electron microscopy (Hitachi, S-800) operated at 15 kV. The chemical composition of the products was analyzed using inductively coupled plasma–optical emission spectroscopy (ICP-OES; LEEMAN LABS).

Electrode was prepared by the Doctor Blade technique by coating of the slurry of 70 wt% $LiMn_2O_4$, 10 wt% of polyvinylidenefluoride (PVdF) as a binder and 20 wt% acetylene black in 1-methyl-2-pyrrolidinone (NMP) onto aluminum foil. Electrochemical measurements were carried out using coin-type cells (CR2032). The cell comprised by a lithium metal electrode and a $LiMn_2O_4$ electrode that were separated by a microporous polypropylene separator. One molar solution of $LiClO_4$ in EC/DEC=1:1 (Tomiyama Pure Chemical) was used as the electrolyte. For the part of the electrochemical tests, $AlPO_4$ (Sigma-Aldrich) was added to the electrolyte in weight ratio electrolyte/$AlPO_4$=1:1. After stirring for 24 h, the solid phase of aluminum phosphate was separated from the electrolyte solution by centrifuge technique. All the cell assembling procedures were done inside the dry box filled with high purity argon. Cycling performance of the cells was studied galvanostatically between 3.5 and 4.3 V on multi-channel battery tester (Hokuto Denko, HJ1010mSM8) for various charge–discharge rates at room temperature, 50 and 60 °C, respectively.

Impedance spectroscopy and cyclic voltammetry measurements were conducted using the Solartron SI 1287 electrochemical interface in the frequency range and voltage region from 0.1 Hz to 1MHz and 3.5 to 4.3 V vs Li^+/Li, respectively. Impedance spectroscopy was measured along with galvanostatic cycling at the charged (4.3 V vs Li^+/Li) and discharged (3.5 V vs Li^+/Li) states. The AC voltage of 10 mV was applied.

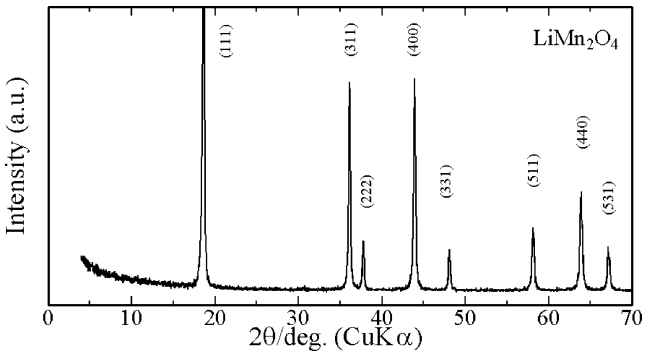

Fig. 1 XRD patterns of nanostructured lithium manganese oxide

Results and discussion

Materials characterization

Figure 1 shows XRD patterns of the $LiMn_2O_4$ samples. The diffraction peaks of samples correspond to a single phase of cubic spinel structure with a space group $Fd\bar{3}m$. The determined lattice parameters of the nanostructured $LiMn_2O_4$ (8.2417 Å) are in good agreement with the theoretical ones [33, 34]. The chemical analysis data have confirmed the stoichiometric composition of the material with good agreement between experimental and theoretical values.

Figure 2 shows typical SEM images of the lithium manganese oxide particles synthesized via ultrasonic spray pyrolysis technique. It can be seen that the particles have spherical shape and porous surface morphology, which is different from the conventional solid state reaction powders with irregular particles shapes [35]. The geometric mean diameter of the $LiMn_2O_4$ powder was about 1.1 μm, and the specific surface area was about 6.6 m^2/g. The crystallite size was about 34 nm.

Electrochemical performance

Figure 3 exhibits the first charge–discharge cycle profiles for the cell Li/1 M $LiClO_4$ in EC/DEC=1:1/$LiMn_2O_4$ at different temperatures and different charge–discharge rates (0.1C and 1C). For all charge–discharge profiles, there are two prolonged plateaus at about 4-V region that is inherent for the lithium insertion-removal at the well-defined lithium manganese spinel structure. The Fig. 3 data show that the nanostructured $LiMn_2O_4$ synthesized in the present work exhibits higher room temperature specific capacity in the 4-V region than the one reported in the literature [32] for as-prepared powders by ultrasonic spray pyrolysis technique. In comparison with the [32] data, in the present work, as-prepared powders have been sintered at 750 °C in air for 4 h. This allowed obtaining the materials with higher crystallinity, which improved the nanostructured cathode performance. The charge and discharge capacity difference, so-called irreversible capacity, is remarkably higher for the high rate experiment especially at 60 °C. This difference would be attributed to the additional energy consumption by the side reactions of the electrolyte oxidation and the surface film formation. One can see that initial discharge capacity decreases with the temperature increase. The data also show an increase in the irreversible capacity at the first cycle when the temperature rises due to the higher ratio of the mentioned side reactions.

Figure 3 also shows that the material has slightly higher capacity for 1C rate experiment than for 0.1C at room temperature. In our previous work [29], the same tendency

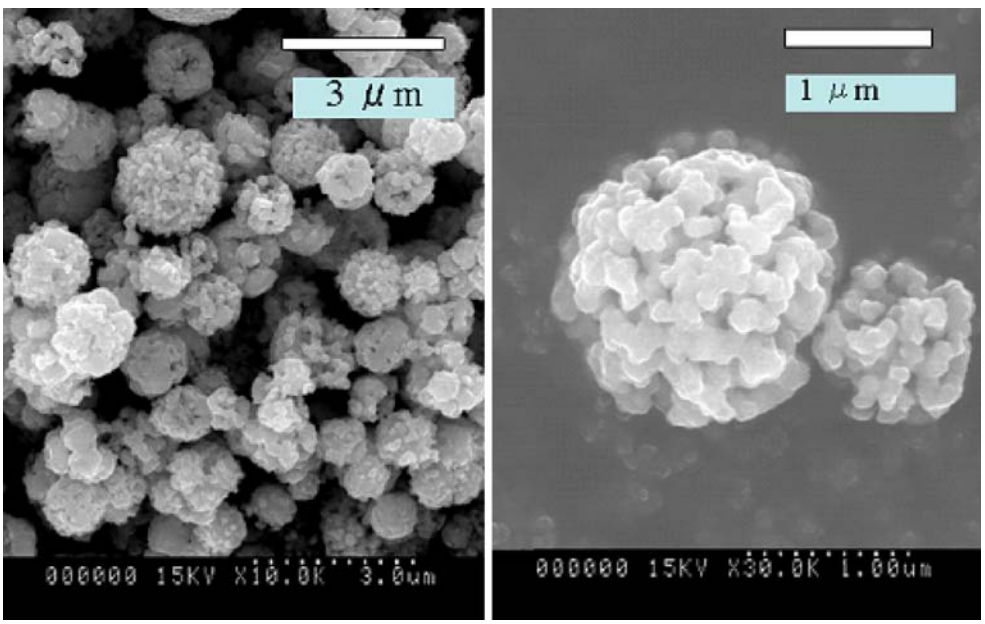

Fig. 2 Typical SEM micrograph of lithium manganese oxide powder with spherical particles

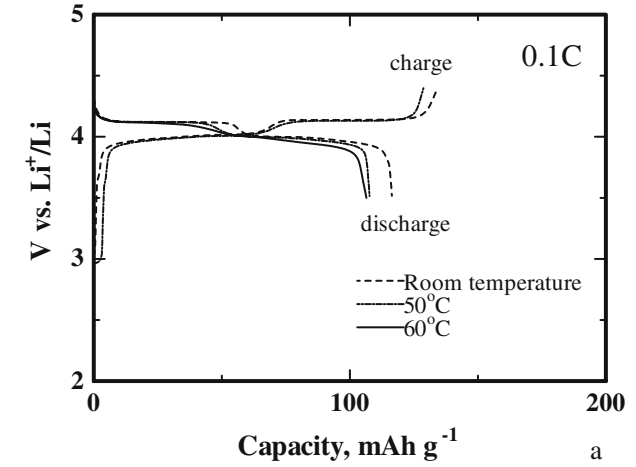

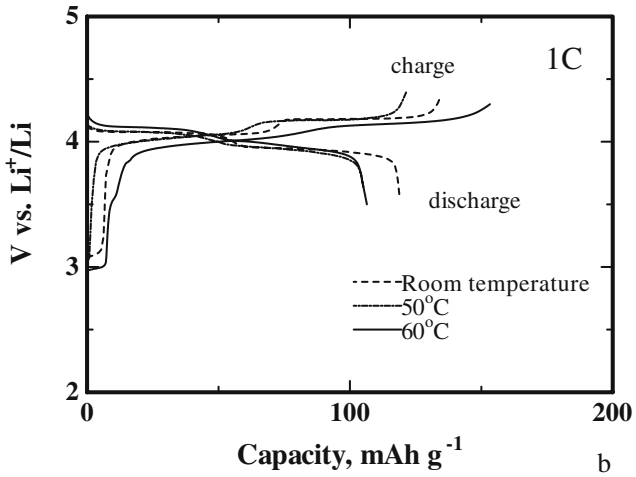

Fig. 3 First charge–discharge cycle profiles for the Li/nanostructured spherical $LiMn_2O_4$ cell at room temperature, 50 °C and 60 °C, **a** 0.1C and **b** 1C charge–discharge rate

was monitored for partially substituted lithium manganese oxides prepared by the ultrasonic spray pyrolysis technique.

In this paper, we show that the nanostructured spherical particle $LiMn_2O_4$ is an excellent candidate for lithium-ion battery cathodes for high electric current application. Figure 4 shows cycling performance of the Li/$LiMn_2O_4$ cell under various charge–discharge rate conditions. It can be seen that the cell with the nanostructured $LiMn_2O_4$ cathode prepared via ultrasonic spray pyrolysis technique exhibits stable cycling even under sever conditions of 10C (1 mA cm^{-2}). In contrast, the non-substituted $LiMn_2O_4$ prepared by usual solid-state reaction method [7] characterized by drastic capacity decay upon cycling.

The data obtained show that the materials synthesized via spray pyrolysis technique are spherical in shape and have porous surface morphology. Previous studies [29–31] have shown that the materials are nanostructured, with narrow particle size distribution and homogeneous composition that provides better conditions for charge transfer. The nanostructured features of the material may account for the enhanced rate performance due to the short diffusion

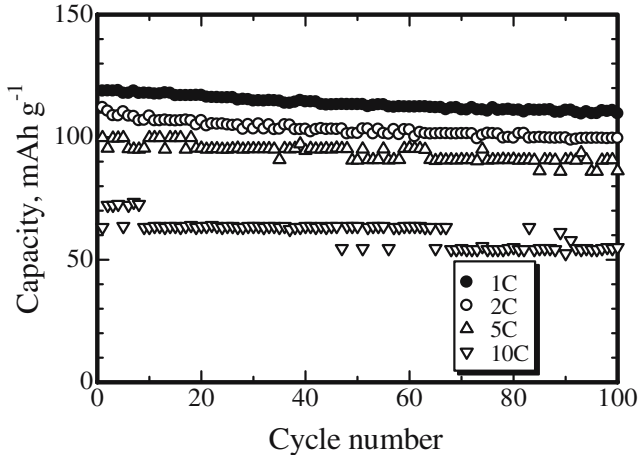

Fig. 4 Room temperature rate capability data for the Li/nanostructured spherical $LiMn_2O_4$ cell

distance of Li^+ in nanostructured electrodes [36, 37]. The high crystallinity and homogeneous chemical composition of lithium manganese oxide $LiMn_2O_4$ synthesized via the ultrasonic spray pyrolysis method with heat treatment may be the reason of the better cycling performance of the nanostructured $LiMn_2O_4$ compared with the one prepared by conventional methods.

Figure 5 illustrates cyclability of the nanostructured $LiMn_2O_4$ electrode at 1C charge–discharge rate at room temperature and at elevated temperatures. It can be seen that the present spherical particles of lithium manganese oxide exhibit good capacity retention, although it cycled at temperatures up to 50 °C under high charge–discharge rate. The capacity continuously decayed when the temperature was increased up to 60 °C. The capacity loss during 50 cycles at this temperature was about 50% from the initial value. This value is about 5 and 12% at room temperature and at 50 °C, respectively.

To improve the electrochemical performance at elevated temperature, the additives of $AlPO_4$ to the electrolyte have

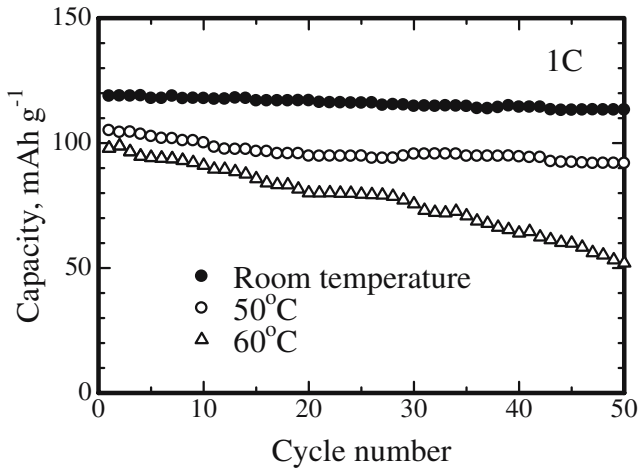

Fig. 5 Discharge capacity retention of Li/nanostructured spherical $LiMn_2O_4$ cell under 1C rate at different temperature conditions

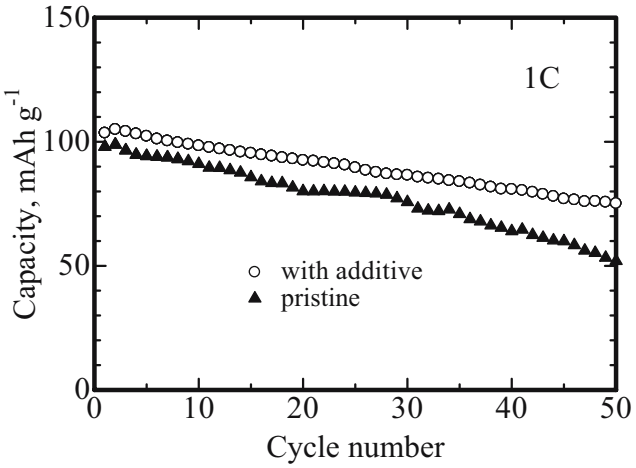

Fig. 6 Effect of $AlPO_4$ electrolyte additives to the capacity retention of the Li/nanostructured spherical $LiMn_2O_4$ cell at 60 °C, 1C

been applied. Figure 6 shows the comparison data on the cell cyclability at 1C charge–discharge rate at 60 °C with and without addition of aluminum phosphate to the electrolyte. Figure 6 shows clear positive effect of the $AlPO_4$ additives on the capacity retention of the system. The capacity loss value has been decreased for almost two times for the aluminum phosphate additive in the electrolyte. In this case, the value of the discharge capacity loss from the initial capacity upon 50 cycles is about 28% against about 50% of the capacity loss when $AlPO_4$ was not added to the system. The addition of $AlPO_4$ to the electrolyte improves the cell capacity retention at elevated temperature for almost two times.

The influence of the $AlPO_4$ additives to the electrode–electrolyte interface was investigated by means of AC impedance spectroscopy.The impedance data obtained for the charged and discharges states of the cell have shown the same trends. The impedance spectroscopy data for the pristine and aluminum phosphate added systems at the charged state are shown in Fig. 7. In the in-boxes, the high frequency parts of the first charged state spectra are given. The graph shows two semicircles in high and medium frequencies (HF and MF, respectively). Small HF semicircles are ascribed to the electrode–electrolyte interface impedance. They are followed by large MF semicircles attributed to the charge transfer resistance. Although the ICP-OES measurements did not detect noticeable amount of aluminum in the electrolyte, one can see that there is a clear evidence of the effect of the aluminum phosphate additives to the cell impedance development during cycling. Considering the average particle size of $AlPO_4$ about 7.5 μm (determined from the SEM data, not shown), it may be suggested that the solid $AlPO_4$ particles were separated from the liquid phase by centrifuge technique, and a residual amount of the dissolved $AlPO_4$ remains in the liquid electrolyte and affects the interfacial processes.

The addition of the aluminum phosphate suppresses the total impedance development of the cell. Figure 7a shows that the impedance changes at the initial part of cycling of the $AlPO_4$ added cell, and the further operation does not lead to progressive changes in the impedance on the prolonged cycling. The impedance behavior of the system without the aluminum phosphate additives is different as shown in Fig. 7b. The pristine cell impedance progresses upon prolonged cycling (Fig. 7b). The impedance of the 30th cycle for the pristine cell is twice higher than that of the 10th cycle, and it rises upon further cycling. These

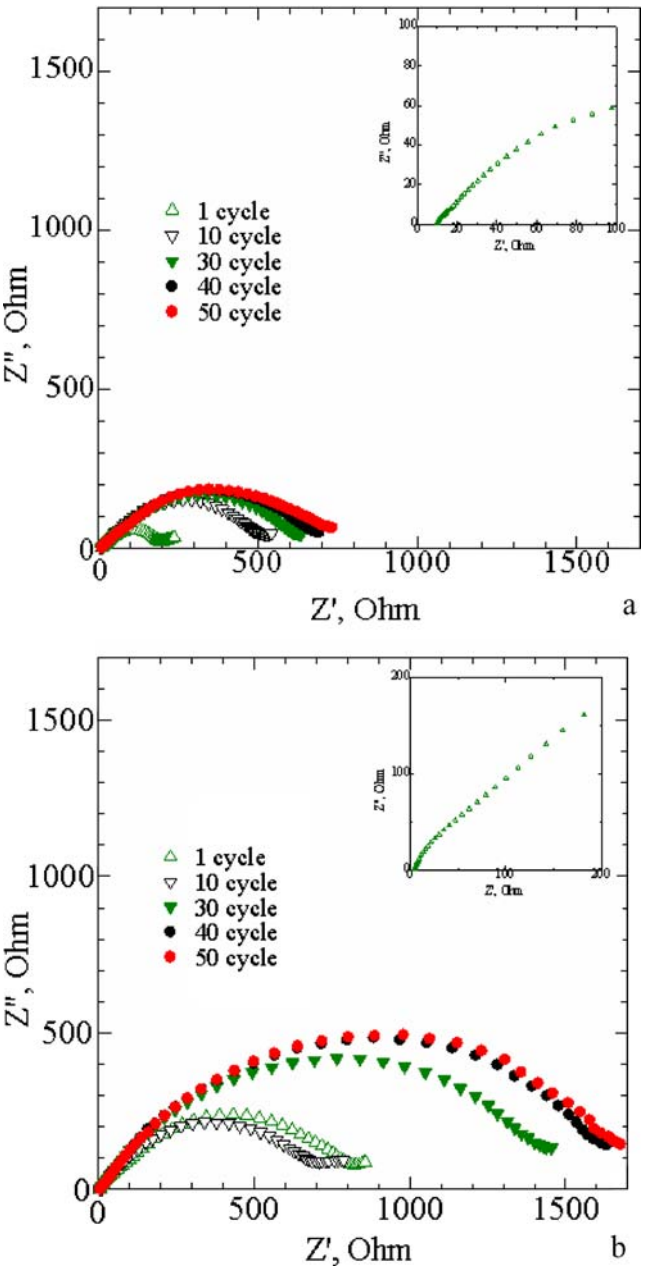

Fig. 7 Impedance spectra of the Li/nanostructured spherical $LiMn_2O_4$ cell with 1M $LiClO_4$ in EC/DEC=1:1 electrolyte at 60 °C **a** with addition of $AlPO_4$ and **b** without addition of $AlPO_4$. *In boxes* High-frequency part of one cycle

results would be attributed to the beneficial effects of the $AlPO_4$ additives such as reduced electrolyte decomposition and a decreased thickness of the SEI as a result, which may lead to the improved interparticle charge transfer. It means that even residual amounts of this additive leads to the stabilization of the film on the electrode surface after its formation at the initial cycles. It is obviously correlated to the electrochemical performance data of Fig. 6. Therefore, the role of the $AlPO_4$ additives to the electrolyte may account for the improved capacity retention of the nanostructured $LiMn_2O_4$ electrode synthesized via ultrasonic spray pyrolysis technique.

The impedance spectroscopy measurements data are in good agreement with the cycling performance data. The addition of aluminum phosphate improves the cell cyclability through the stabilization of the electrode surface and prevention of its change upon prolonged cycling. The elucidation of the thin SEI layer on the electrode surface in the system with addition of $AlPO_4$ is needed.

Conclusion

The nanostructured lithium manganese oxide with spherical shape of particles synthesized via ultrasonic spray pyrolysis technique exhibited stable cycling performance at room temperature up to 10C charge–discharge rate tests. The electrochemical performance of the nanostructured $LiMn_2O_4$ prepared in this work is superior to the material prepared by conventional methods.

The temperature increase leads to the lowering of the cell capacity. Cycling performance of the $Li/LiMn_2O_4$ cell at 50 °C (1C) rate is characterized by 12% of the initial capacity loss after 50 cycle tests. For the same construction of the cell, this value increases up to 50% at 60 °C. Application of the aluminum phosphate additives to the electrolyte allows reducing the initial capacity loss by two times. During the charge–discharge tests over 50 cycles at 1C rate condition, the cell loses about 28% of the initial capacity. The impedance spectroscopy data confirmed the positive effect of the aluminum phosphate additive to the cell performance. The observed data allow the suggestion that the improvement of the cell performance at elevated temperature is mainly due to the stabilization of the electrode–electrolyte interface by the aluminum phosphate additive that suppresses the increase in the interface impedance during prolonged cycling.

Ultrasonic spray pyrolysis technique allows the preparation of the nanostructured non-doped $LiMn_2O_4$ with spherical particles which has perspectives for the utilization as a cathode for high rate and elevated temperature applications. The aluminum phosphate addition to the electrolyte might be considered as one of the ways for the improvement of the elevated temperature performance of the lithium manganese oxide-based batteries.

Acknowledgments The authors thank Prof. M. Nakayama from Department of Applied Chemistry, Tokyo Institute of Technology, for helpful discussions and technical support of some experimental works.

References

1. Aricò AS, Bruce P, Scrosati B, Tarascon JM, van Schalkwijk W (2005) Nature Materials 4:366
2. Okamoto E (2002) ASAIO J 48(5):495–502
3. Alper J (2002) Science 296:1224
4. Wakihara M (2001) Mater Sci Eng R33:109
5. Takamura T (2002) Solid State Ionics 152–153:19
6. Tarascon JM, McKinnon WR, Goowar F, Bowmer TN, Amatucci G, Guyomard D (1994) J Electrochem Soc 141:1421
7. Li G, Ikuta H, Uchida T, Wakihara M (1996) J Electrochem Soc 143:178
8. Pistoia G, Zane D, Zhang Y (1995) J Electrochem Soc 142:2551
9. Blyr A, Sigala C, Amatucci G, Guyomard D, Chabre Y, Tarascon JM (1998) J Electrochem Soc 145:194
10. Xia Y, Kumada N, Yoshio M (2000) J Power Sources 90:135
11. Palacı´n MR, Chabre Y, Dupont L, Hervieu M, Strobel P, Rousse G, Masquelier C, Anne M, Amatucci GG, Tarascon JM (2000) J Electrochem Soc 147:845
12. Shu D, Chung KY, Cho WI, Kim KB (2003) J Power Sources 114:253
13. Xia Y, Zhou Y, Yoshio M (1997) J Electrochem Soc 144:2593
14. Shao-Horn Y, Hackney SA, Kahaian AJ, Kepler KD, Skinner E, Vaughey JT, Thackeray MM (1999) J Power Sources 81–82:496
15. Gummow RJ, de Kock A, Thackery MM (1994) Solid State Ionics 69:59
16. Ma S, Noguchi N, Yoshio M (2001) J Power Sources 97–98:385
17. Wu SH, Su HJ (2002) Mater Chem Phys 78:189
18. Shaju KM, Rao GVS, Chowdari BVR (2002) Solid State Ionics 148:343
19. Kannan AM, Manthiram A (2002) Electrochem Solid State Lett 5: A167
20. Cho J, Kim GB, Lim HS, Kim CS, Yoo SI (1999) Electrochem Solid State Lett 2:607
21. Sun YK, Lee YS, Yoshio M, Amine K (2002) Electrochem Solid State Lett 5:A99
22. Liu Z, Wang H, Fang L, Lee JY, Gan LM (2002) J Power Sources 104:101
23. Chen Z, Dahn JR (2002) Electrochem Solid State Lett 5:A213
24. Myung ST, Izumi K, Komaba S, Sun YK, Yashiro H, Kumagai N (2005) Chem Mater 17:3695
25. Gnanaraj JS, Pol VG, Gedanken A, Aurbach D (2003) Electrochem Comm 5:940
26. Tu J, Zhao XB, Xie J, Cao GS, Zhuang DG, Zhu TJ, Tu JP (2007) J Alloys Compnd 432:313
27. Cho J, Kim YW, Kim B, Lee JG, Park B (2003) Angew Chem Int Ed 42:1618
28. Kim B, Kim C, Kim TG, Ahn D, Park B (2006) J Electrochem Soc 153:A1773
29. Bakenov Zh, Taniguchi I (2005) Solid State Ionics 176:1027
30. Taniguchi I, Bakenov Z (2005) Powder Technol 159:55
31. Taniguchi I (2005) Mater Chem Phys 92:172
32. Park S, Myung S, Oh S, Yoon C, Sun Y (2006) Electrochim Acta 51:4089
33. Song D, Ikuta H, Uchida T, Wakihara M (1999) Solid State Ionics 117:151
34. Ohzuku T, Kitagawa M, Hirai T (1990) J Electrochem Soc 137:769
35. Wang Z, Ikuta H, Uchimoto Y, Wakihara M (2003) J Electrochem Soc 150(9):A1250
36. Im D, Manthiram A (2003) J Electrochem Soc 150:A742
37. Im D, Manthiram A (2002) J Electrochem Soc 149:A1001